Creep of the matrix during coalescence and overgrowth of graphite precipitates in a high-silicon spheroidal graphite iron submitted to thermal cycling in the ferritic domain.

Tito Andriollo[1], Jacques Lacaze[2*], Niels Tiedje[1]

1- Department of Mechanical Engineering, Technical University of Denmark, Anker Engelunds Vej 101A, Kgs. Lyngby, 2800, Denmark

2- CIRIMAT, Université de Toulouse, 4 allée Monso, BP 44362, 31030 Toulouse cedex 4, France

Corresponding author: Jacques Lacaze, Jacques.lacaze@ensiacet.fr

Abstract

Thermal cycling of a high-silicon spheroidal graphite cast iron within the ferritic domain leads to coalescence of graphite particles with dendritic protuberances on the largest ones. This phenomenon occurs if there is some dissolution of graphite at the maximum temperature of the thermal cycle. Upon cooling, carbon redeposits in preferred locations, leading to the protuberances. This communication demonstrates that the ferritic matrix around the overgrowths can creep and remain in close contact with graphite.

Thermal cycling of a high-silicon spheroidal graphite cast iron within the ferritic domain has recently been shown to lead to marked coalescence of graphite particles with the development of dendritic protuberances on the largest ones [1]. The alloy which was investigated consisted of 3.10 wt.% carbon, 4.45 wt.% silicon, 0.25 wt.% manganese and 0.0037 wt.% antimony (Fe balance) and had an as-cast fully ferritic matrix stable up to 850°C as verified with differential thermal analysis. Samples 2·10·10 mm^3 were subjected to thermal cycles which were each 480 seconds long and included a hold at 800°C±10°C for 60 seconds. The evolution of the microstructure was investigated after 1000, 2000 and 3000 cycles, this later value corresponding to a cumulative length of time at 800°C of 50 hours. Comparing the microstructure of the as-cast material in figure 1-a and after 2000 cycles in

figure 1-b illustrates the marked coalescence undergone by the graphite precipitates. Figure 1-c shows at higher magnification that growth of the large precipitates proceeds by the development of dendrite-like protuberances instead of a homogeneous increase of the diameter of the spheroids.

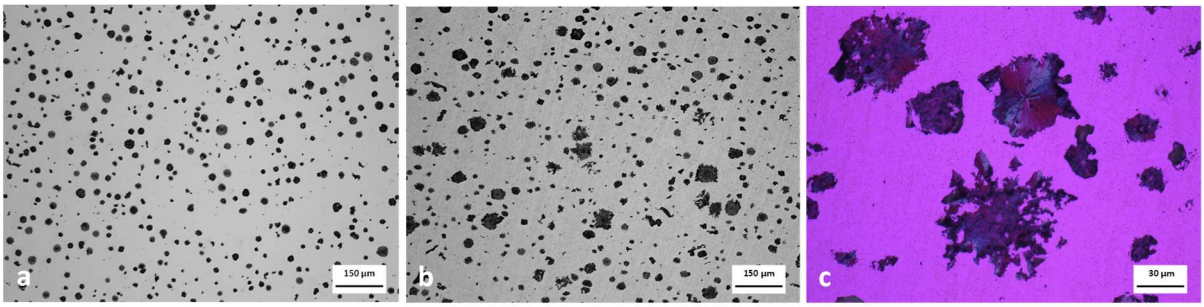

Figure 1 – Light optical micrographs of the initial microstructure (a), of the microstructure after 2000 thermal cycles (b) and detail of dendritic overgrowths under polarized light (c).

Coalescence of the graphite particles is expected to occur provided the maximum temperature reached during the thermal cycles is high enough for some dissolution of graphite to occur. Upon cooling, carbon is seen to re-deposit in selected locations as protuberances rather than homogeneously around the largest particles. This schematic would imply the formation of a gap between the graphite particles and the surrounding matrix upon heating as carbon dissolves within ferrite. Upon cooling, it would be expected that this gap remains in locations where carbon does not re-precipitate. With cycling, dendritic protuberances grow and the gap would thus have enlarged which is not observed. As a matter of fact, the ferritic matrix appears in close contact of graphite all around the precipitates. This suggests that creep of the matrix occurred at a rate that was sufficient for the gap to be closed even where carbon does not redeposit. The aim of this work was thus to model the creep of ferrite occurring while a graphite protrusion develops due to the inhomogeneous precipitation of carbon during successive thermal cycles.

Inspired by previous micro-mechanical studies of spheroidal graphite cast iron [2,3], a unit cell containing a single graphite spheroid was considered, see figure 2-a. The spheroid is initially spherical with radius R_0 and it is embedded in a cylinder of ferrite with initial height $2 \cdot L_0$ and initial radius L_0. The value of L_0 was set to $1.88 \cdot R_0$, such that the graphite volume fraction of the unit cell is equal to 10 %. The deformation of the unit cell was simulated via a 2D axisymmetric finite element model corresponding to the area enclosed by

the yellow dashed line in figure 2-a. In the model, the coordinate along the symmetry axis was labelled z and the coordinate along the radial axis was labelled r. Note that the origin of the coordinates coincides with the center of the spheroid and of the entire unit cell.

During thermal cycling, the shape of the spheroid changes due to the carbon dissolution and subsequent inhomogeneous precipitation. In order to avoid modelling each individual cycle, it was assumed that the result of this dissolution and precipitation process is an isochoric geometrical transformation of the spheroid, i.e. the spheroid changes shape while keeping the same volume. This geometric transformation is described by the movement of the points along the matrix-graphite interface according to the following displacement functions:

$$\begin{cases} u_r(r,z) = -\eta(z)\cdot\epsilon_z\cdot r + \big(1-\eta(z)\big)\cdot\tilde{l}(\epsilon_z) \\ u_z(r,z) = -\eta(z)\cdot\epsilon_z\cdot z \end{cases} \quad (1)$$

With

$$\eta(z) = \frac{1}{2}\left(1+\cos\left(\pi\cdot\left(1-\frac{z}{R_0}\right)^m\right)\right) \quad (2)$$

In the above expressions, m is a shape parameter controlling the width of the protrusion (set to 5) and ϵ_z is the variable representing the relative contraction of the spheroid along the z axis. The quantity $\tilde{l}$ corresponds to the length of the protrusion and it is computed, for a given value of ϵ_z, based on the spheroid volume conservation by exploiting Pappus' theorem for solids of revolution. The evolution of the geometric transformation with time t was assumed to be dictated by the following linear law:

$$\epsilon_z = c\cdot t \quad (3)$$

where the proportionality factor c was set to $2\cdot10^{-3}$ h^{-1}. This value implies that during a time interval of 50 hours – which corresponds to the maximum number of cycles experimentally investigated [1] – the spheroid contracts by 10 % along the z-axis and, simultaneously, an annular protrusion $\approx 0.5\cdot R_0$ long grows in the direction of the r-axis. The evolution of the spheroid shape over time is depicted graphically in figure 2-b.

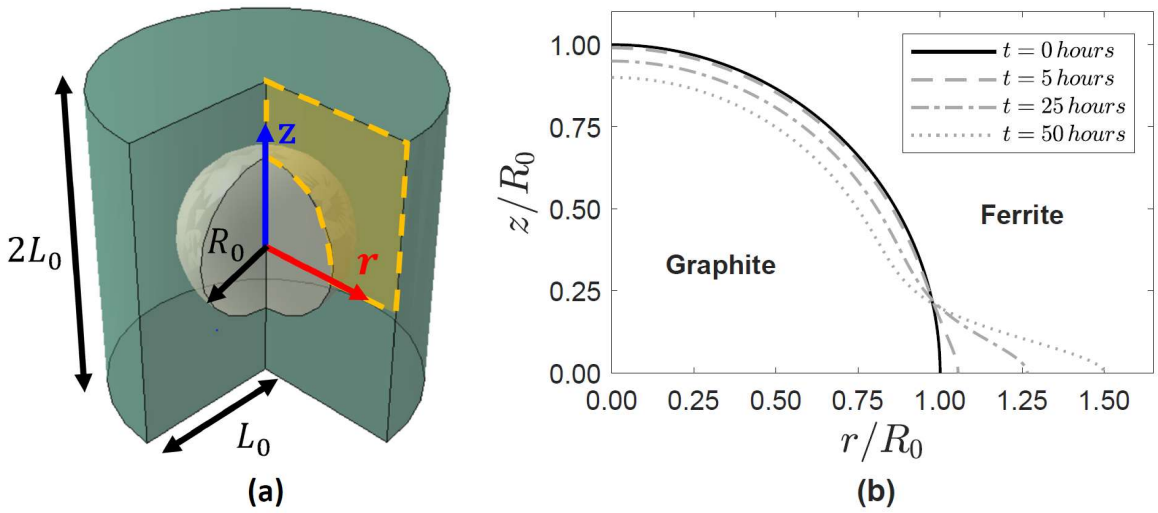

Figure 2 – (a) Axisymmetric unit cell used to study the creep of the ferrite around the graphite. (b) Time evolution of the spheroid shape according to Eqs. 1-3.

The domain of the finite element model, shown in figure 2-a, was discretized with a mesh consisting of ≈ 10000 axisymmetric 4-node elements. Symmetry boundary conditions were imposed along the boundaries corresponding to $z = 0$ and $r = 0$ and periodic boundary conditions were prescribed along the boundaries corresponding to $z = L_0$ and $r = L_0$ [4]. The deformation of ferrite, which was assumed to occur at a constant temperature of 800ºC, was simulated by prescribing the motion of the nodes along the graphite-ferrite interface according to Eqs. 1-3. Due to the severe mesh distortion associated with the formation of the protuberance, manual remeshing was performed at regular intervals during the numerical simulation.

The ferritic matrix was assumed to obey the visco-plastic constitutive model described in detail in Andriollo et al. [5]. It is worth remarking that the present material contains a higher Si concentration (4.45 wt.%) than the alloys used calibrate the former model (2-3 wt.%). Therefore, the model is likely to overestimate somewhat the creep of ferrite in the present case. In this respect, Davies |6] determined the activation energy H for steady-state creep of ferrite above 500 ºC as a function of the Si content up to 5 wt.%. According to these authors, the steady-state creep rate $\dot{\varepsilon}$ is related to H and to the applied stress σ as follows:

$$\dot{\varepsilon} \propto \sigma^n \cdot \exp(-H/R \cdot T) \qquad (4)$$

where n is the creep exponent, T is the absolute temperature and R is the gas constant. Based on Eq. 4 and on the values of H reported in [6], an increase of ≈ 1.5 wt.% in the ferrite Si concentration can be expected to decrease the creep rate by a factor ≈ 2 for a given applied stress, or to increase the stress by a factor ≈ $2^{1/n}$ for a given creep rate. At temperature above 600°C which was the highest investigated by Davies, the changes due to silicon content are expected to decrease.

Figure 3 shows the contours of the von Mises stress in the ferritic matrix at different times, as predicted by the finite element model. Time 0 corresponds to the beginning of the deformation process from an initial unstressed state at 800°C. The peak values are localized ahead of the protuberance and increase from ≈ 10 MPa to ≈ 17 MPa as the protuberance develops over time. This appears to be a localized effect associated with the increasing curvature of the protuberance tip, which enhances the stress concentration in the nearby ferrite. Indeed, the size of the region where the von Mises stress is larger than 7 MPa (green, yellow and red colors) seems to remain approximately constant over time. The other stress measures (maximum principal stress, hydrostatic stress, etc.) are of the same order of magnitude than the von Mises stress. The graphite spheroid is probably capable of sustaining these stresses without breaking up, as the compressive strength of isotropic graphite used in nuclear application is usually no less than 50 MPa at room temperature and varies very little with temperature up to ≈ 1100 ºC [7].

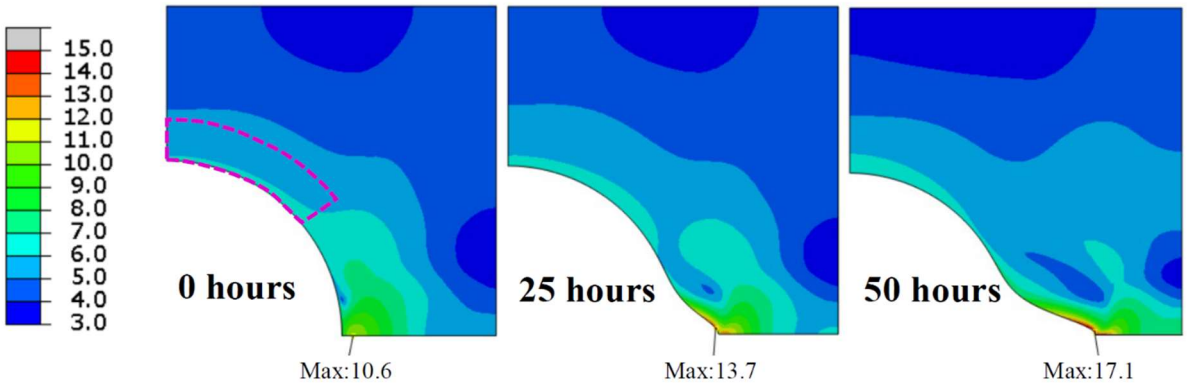

Figure 3 – Contours showing the evolution of the von Mises stress in ferrite over time, values are in MPa.

The evolution of the equivalent strain rate is reported in figure 4. The order of magnitude near the tip of the protuberance is 10^{-5} s^{-1} at the beginning of the deformation and increases

by a factor ≈ 7 after 50 hours. Overall, the strain rate is within the range of validity of the visco-plastic model used to simulate the creep of the ferrite matrix [5]. It is worth noting that the different appearance of the contours of figure 3 and those of figure 4 is a consequence of the creep exponent n (see Eq. 4) which, based on the predicted stresses and strain rates, can be expected to lie between 3 and 4 [8]. This relatively large value of the creep exponent greatly enhances the strain rate gradients compared to the corresponding stress gradients.

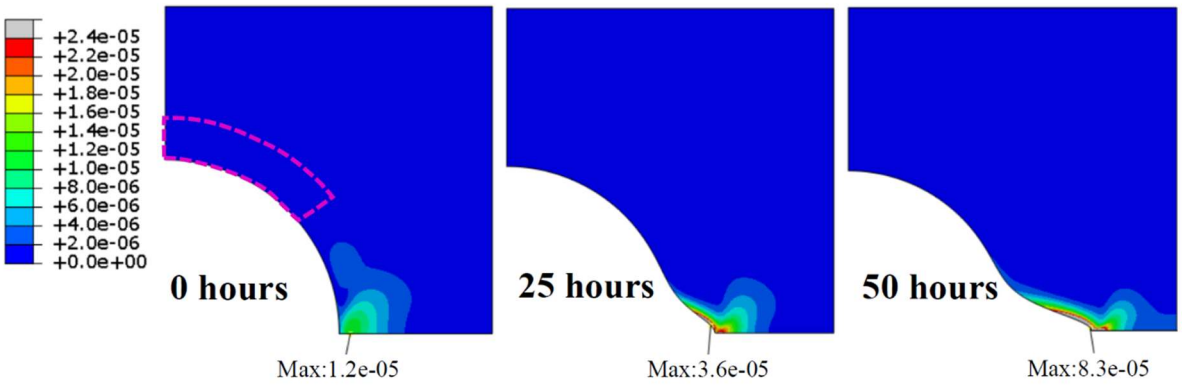

Figure 4 – Contours showing the evolution of the equivalent strain rate in the ferrite over time, values are in s^{-1}.

In order to investigate deeply the creep of ferrite near the location where the gap would be expected to form, the mean values of the von Mises stress σ_{eq}^{avg} and strain rate $\dot{\varepsilon}_{eq}^{avg}$ are computed over the region localized within the purple dashed line in figure 3 and figure 4. Such a region is defined by the points whose distance from the graphite is less than $0.2 \cdot R_0$ and whose value of the ratio z/r is greater than one. Figure 5 shows that σ_{eq}^{avg} and $\dot{\varepsilon}_{eq}^{avg}$ remain essentially stable as the protuberance grows and are in the order of ≈ 6 MPa and ≈ $1 \cdot 10^{-6}$ s^{-1}, respectively. Even considering the model overestimation of the ferrite creep discussed previously, these values seem very reasonable when compared to the results of steady-state creep tests conducted at similar temperatures |8-10]. Therefore, it can be concluded that the amount of creep required for maintaining the ferritic matrix in contact with the graphite precipitate during formation of the protuberance can be effectively achieved.

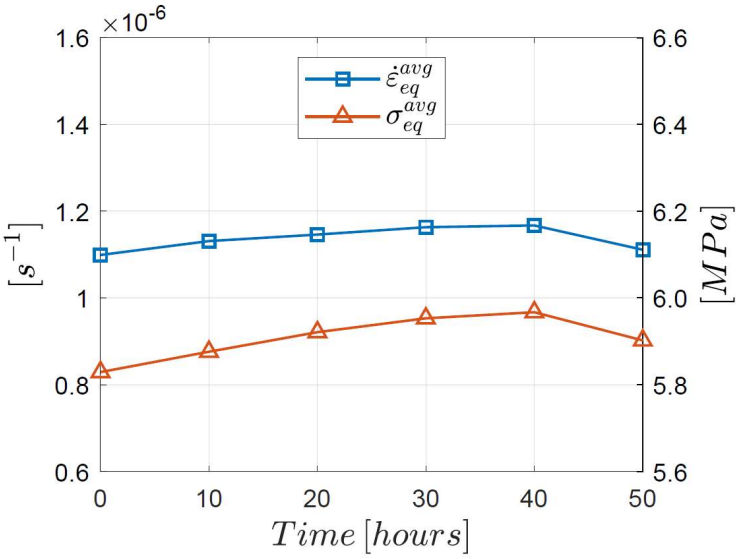

Figure 5 – Time evolution of the average value of the equivalent strain rate ($\dot{\varepsilon}_{eq}^{avg}$) and von Mises stress ($\sigma_{eq}^{avg}$) in the ferrite region where the gap would be expected to develop (see the text for the precise definition).

Acknowledgements

This work was partially carried out within the frame of the project ‘‘Optimised high performance ductile cast iron using 4D X-ray analysis and microstructural modelling’’, Danish Research Council for Independent Research, grant no. 10-093966.

References

[1] A. Ebel, M. Alves Pegoraro, B. Malard, C. Tenailleau and J. Lacaze: Scr. Mater., 2020, Vol. 178, pp. 86–89.

[2] K.S. Zhang, J.B. Bai and D. François: Int. J. Solids Struct., 1999, Vol. 36, pp. 3407–25

[3] N. Bonora and A. Ruggiero: Int. J. Solids Struct., 2005, Vol. 42, pp. 1401–24.

[4] A. Drago and M. Pindera: Compos. Sci. Technol., 2007, Vol. 67, pp. 1243–63.

[5] T. Andriollo, K. Hellström, M.R. Sonne, J. Thorborg, N. Tiedje and J. Hattel: J. Mech. Phys. Solids, 2018, Vol. 111, pp. 333–57.

[6] R.G. Davies: Trans. Metall. Soc. AIME, 1963, Vol. 227, pp. 665–68.

[7] W.L. Greenstreet, J.E. Smith and G.T. Yahr: Carbon, 1969, Vol. 7, pp. 15–45.

[8] C. Barrett: Trans. Metall. Soc. AIME, 1967, Vol. 239, pp. 1726–28.

[9] C. Barrett and W. Nix: Acta Metall., 1965, Vol. 13, pp. 1247–58.

[10] R.G. Stang, W.D. Nix and C.R. Barrett: Metall. Trans., 1973, Vol. 4, pp. 1695–99.